Optical properties of strain-compensated CdSe/ZnSe/(Zn,Mg)Se quantum well microdisks

M. Ruth,[1] A. Finke,[1] G. Schmidt,[1,2] D. Reuter,[1] S. Scholz,[3] A. Ludwig,[3] A. D. Wieck,[3] and A. Pawlis[1,2,*]

[1] *University of Paderborn, Warburger Str. 100, 33098 Paderborn, Germany*
[2] *Peter Grünberg Institut (PGI-9), Forschungszentrum Jülich GmbH, Leo-Brandt-Straße, 52425 Jülich, Germany*
[3] *Ruhr-Universität Bochum, Universitätsstraße 150, 44780 Bochum, Germany*
[*] *a.pawlis@fz-juelich.de*

Abstract: Strain-compensated CdSe/ZnSe/(Zn,Mg)Se quantum well structures that were grown on (In,Ga)As allow for efficient room-temperature photoluminescence and spectral tuning over the whole visible range. We fabricated microdisk cavities from these samples by making use of a challenging chemical structuring technique for selective and homogeneous removal of the (In,Ga)As sacrificial layer below the quantum structure. The observed whispering gallery modes in our microdisks are mainly visible up to photon energies of ~ 2.3 eV due to strong self-absorption. As extinction coefficients and effective refractive indices are dominated by the quantum well material CdSe, thick quantum wells (> 3 monolayer) are necessary to observe resonances in the corresponding quantum well emission.

OCIS codes: (160.6000) Semiconductor materials; (230.5590) Quantum-well, -wire and -dot devices; (220.4000) Microstructure fabrication; (260.3800) Luminescence.

References and links

1. F. Gindele, U. Woggon, W. Langbein, J. M. Hvam, K. Leonardi, D. Hommel, and H. Selke, "Excitons, biexcitons, and phonons in ultrathin CdSe/ZnSe quantum structures," Phys. Rev. B **60**, 8773–8782 (1999).
2. T. -Y. Chung, J. H. Oh, S. -G. Lee, J. -W. Jeong, and K. J. Chang, "Optical properties of ZnSSe/ZnMgSSe quantum wells," Semicond. Sci. Tech. **12**(6), 701–707 (1997).
3. A. V. Platonov, V. P. Kochereshko, D. R. Yakovlev, U. Zehnder, W. Ossau, W. Faschinger, and G. Landwehr, "Optical studies of ZnSe/ZnMgSSe-based quantum-well semiconductor heterostructures," Phys. Solid State **40**(5), 745–746 (1998).
4. A. Pawlis, A. Khartchenko, O. Husberg, D. J. As, K. Lischka, and D. Schikora, "Large room temperature Rabi-splitting in a ZnSe/(Zn,Cd)Se semiconductor microcavity structure," Solid State Comm. **123**(5), 235–238 (2002).
5. A. Curran, J. K. Morrod, K. A. Prior, A. K. Kar, and R. J. Warburton, "Exciton-photon coupling in a ZnSe-based microcavity fabricated using epitaxial liftoff," Semicond. Sci. Tech. **22**(11), 1189–1192 (2007).
6. K. Sebald, M. Seyfried, S. Klembt, S. Bley, A. Rosenauer, D. Hommel, and C. Kruse, "Strong coupling in monolithic microcavities with ZnSe quantum wells," Appl. Phys. Lett. **100**(16), 161104 (2012).
7. M. Klude, T. Passow, R. Kroger, and D. Hommel, "Electrically pumped lasing from CdSe quantum dots," Electron. Lett. **37**(18), 1119–1121 (2001).
8. K. Sebald, P. Michler, T. Passow, D. Hommel, G. Bacher, and A. Forchel, "Single-photon emission of CdSe quantum dots at temperatures up to 200 K," Appl. Phys. Lett. **81**(16), 2920–2922 (2002).
9. A. Tribu, G. Sallen, T. Aichele, R. André, J. -P. Poizat, C. Bougerol, S. Tatarenko, and K. Kheng, "A high-temperature single-photon source from nanowire quantum dots," Nano Letters **8**(12), 4326–4329 (2008).

#246877 Received 28 Jul 2015; revised 24 Sep 2015; accepted 24 Sep 2015; published 29 Oct 2015

10. S. Bounouar, M. Elouneg-Jamroz, M. D. Hertog, C. Morchutt, E. Bellet-Amalric, R. André, C. Bougerol, Y. Genuist, J. -P. Poizat, S. Tatarenko, and K. Kheng, "Ultrafast room temperature single-photon source from nanowire-quantum dots," Nano Letters **12**(6), 2977–2981 (2012).
11. S. Nakamura, "The roles of structural imperfections in InGaN-based blue light- emitting diodes and laser diodes," Science **281**(5379), 956–961 (1998).
12. R. W. Martin, P. R. Edwards, R. Pecharroman-Gallego, C. Liu, C. J. Deatcher, I. M. Watson, and K. P. O'Donnell, "Light emission ranging from blue to red from a series of InGaN/GaN single quantum wells," J. Phys. D **35**(7), 604–608 (2002).
13. B. Damilano and B. Gil, "Yellow-red emission from (Ga,In)N heterostructures," J. Phys. D **48**, 403001 (2015).
14. M. H. Crawford, "LEDs for solid-state lighting: Performance challenges and recent advances," IEEE J. Sel. Top. Quant. Electron. **15**, 1028–1040 (2009).
15. Y. J. Hong, C. -H. Lee, A. Yoon, M. Kim, H. -K. Seong, H. J. Chung, C. Sone, Y. J. Park, and G. -C. Yi, "Visible-color-tunable light-emitting diodes," Adv. Mat. **23**(29), 3284–3288 (2011).
16. Y. -H. Ko, J. -H. Kim, S. -H. Gong, J. Kim, T. Kim, and Y. -H. Cho, "Red emission of InGaN/GaN double heterostructures on GaN nanopyramid structures," ACS Photonics **2**(4), 515–520 (2015).
17. D. Simeonov, E. Feltin, A. Altoukhov, A. Castiglia, J. -F. Carlin, R. Butté, and N. Grandjean, "High quality nitride based microdisks obtained via selective wet etching of AlInN sacrificial layers," Appl. Phys. Lett. **92**, 171102 (2008).
18. M. Athanasiou, R. Smith, B. Liu, and T. Wang, "Room temperature continuous-wave green lasing from an InGaN microdisk on silicon," Scientific Reports **4**, 7250 (2014).
19. A. Finke, M. Ruth, S. Scholz, A. Ludwig, A. D. Wieck, D. Reuter, and A. Pawlis, "Extending the spectral range of CdSe/ZnSe quantum wells by strain engineering," Phys. Rev. B **91**(3), 035409 (2015).
20. A. Pawlis, M. Panfilova, K. Sanaka, T. D. Ladd, D. J. As, K. Lischka, and Y. Yamamoto, "Low-threshold ZnSe microdisk laser based on fluorine impurity bound-exciton transitions," Microelectr. J. **40**(2), 256–258 (2009).
21. K. Sanaka, A. Pawlis, T. D. Ladd, K. Lischka, and Y. Yamamoto, "Indistinguishable photons from independent semiconductor nanostructures," Phys. Rev. Lett. **103**(5), 053601 (2009).
22. K. De Greve, S. M. Clark, D. Sleiter, K. Sanaka, T. D. Ladd, M. Panfilova, A. Pawlis, K. Lischka, and Y. Yamamoto, "Photon antibunching and magnetospectroscopy of a single fluorine donor in ZnSe," Appl. Phys. Lett. **97**(24), 241913 (2010).
23. K. Sanaka, A. Pawlis, T. D. Ladd, D. J. Sleiter, K. Lischka, and Y. Yamamoto, "Entangling single photons from independently tuned semiconductor nanoemitters," Nano Letters **12**(9), 4611–4616 (2012).
24. K. Pinardi, U. Jain, S. C. Jain, H. E. Maes, R. Van Overstraeten, and M. Willander, "Critical thickness and strain relaxation in lattice mismatched II-VI semiconductor layers," J. Appl. Phys. **83**(9), 4724–4733 (1998).
25. D. Schikora, S. Schwedhelm, D. J. As, K. Lischka, D. Litvinov, A. Rosenauer, D. Gerthsen, M. Strassburg, A. Hoffmann, and D. Bimberg, "Investigations on the Stranski-Krastanow growth of CdSe quantum dots," Appl. Phys. Lett. **76**(4), 418–420 (2000).
26. M. Ruth, T. Zentgraf, and C. Meier, "Blue-green emitting microdisks using low temperature-grown ZnO on patterned silicon substrates," Optics Express **21**(21), 25517–25525 (2013).
27. X. Liu and J. K. Furdyna, "Optical dispersion of ternary II-VI semiconductor alloys," J. Appl. Phys. **95**(12), 7754–7764 (2004).

1. Introduction

The wide-gap II-VI semiconductors unify excellent material properties, namely high oscillator strength and exciton binding energy (i.e. exceeding 20 meV in bulk ZnSe) [1] required for optoelectronic applications at room temperature. Moreover, using GaAs substrates, nearly lattice-matched quantum structures for example based on Zn(S,Se) and (Zn,Mg)(S,Se) can be grown by molecular beam epitaxy (MBE) [2, 3]. Referring to these excellent properties, optically-pumped or low-current devices which include microcavity implementations are still of significant basic and applied research interest. Among them room-temperature polariton emitters [4–6], CdSe quantum dot lasers [7] and single-photon sources [8–10] were demonstrated by different research groups.

Within the common material spectrum only GaN and (In,Ga)N based quantum well and quantum dot structures, which have strongly advanced in the last decades [11–13], provide similar features and even slightly higher binding energies. However, accessing the long wavelength range (green-yellow and red emission) is still a challenge with simple (In,Ga)N QWs due to the enlarged internal electric field and poor crystal quality with high indium content [14]. Advanced and complex nanostructures, such as nano-rods in combination with electrical tuning [15] or

#246877 Received 28 Jul 2015; revised 24 Sep 2015; accepted 24 Sep 2015; published 29 Oct 2015

nano-pyramid-arrays [16] have to be fabricated to overcome these problems. Microdisk lasers based on (In,Ga)N QWs have also been so far demonstrated, but the emission bandwith of those is also limited to the blue-green spectrum [17, 18].

In contrast, binary CdSe/ZnSe QWs allow the tuning of the emission nearly over the whole visible spectral range just by varying the thickness of the CdSe QW. Note that as the main advantage, no ternary QW material is required, which would introduce an increased inhomogeneous broadening due to alloy scattering. Especially for integrated-optical devices (e.g. waveguide-coupled microdisks) fabricated from the same sample chip, longer emission wavelength would be preferred to reduce the relatively strong photon re-absorption probability in the ZnSe host crystal starting in the blue spectral range. In this context we have recently established so called "strain-engineered" CdSe/ZnSe/(Zn,Mg)Se QWs grown on (In,Ga)As substrates: Here efficient room- and low-temperature photoluminescence and spectral tunability almost over the whole visible range ($470-600$ nm wavelength) was achieved just by the variation of the CdSe well width between $1-6$ monolayer (ML) [19] .

Low-threshold microdisk lasing based on ZnSe QWs enclosed in (Zn,Mg)Se barriers was demonstrated in 2009 [20]. The key component to achieve the low lasing-threshold was the fluorine doping of the active region, which triggered the lasing on the fluorine-related donor-bound exciton transition. Alternatively, by isolation of single fluorine donors in high-quality ZnSe QWs via advanced nano-fabrication techniques, indistinguishable and scalable single-photon-sources were recently demonstrated [21–23]. For both, low-threshold microdisk lasers and single-photon sources, the emission wavelength is correlated with the ground state emission of the ZnSe QWs, and consequently, limited to the blue spectral range. Exchanging the ZnSe QWs with CdSe QWs may allow the development of similar microdisk lasers and single-photon sources in the longer wavelength region. Therefore, microdisks and nanostructures based on CdSe QWs provide a versatile basis for future integrated-optical quantum devices at least in the yellow to red spectral range for which the absorption losses in ZnSe and (Zn,Mg)Se based waveguides are substantially smaller than in the blue spectral range. In the following, we report on the optical properties and mode structure of first microdisk cavities fabricated from the above mentioned strain-compensated CdSe/ZnSe/(Zn,Mg)Se QWs.

2. Experimental details

All samples presented in this work were grown by MBE on (001)-GaAs substrates covered with an about $2\,\mu$m thick (In,Ga)As layer with $12-14$ % indium concentration. These thick (In,Ga)As layers are nearly fully relaxed on the GaAs, which allows to deposit the (Zn,Mg)Se barrier layers of our quantum structures with $10-12$ % magnesium concentration lattice-matched on top of the (In,Ga)As quasi-substrates. Single CdSe QWs with a various width between $1-6$ ML were embedded in $2-3$ nm thick ZnSe cladding layers and enclosed in the (Zn,Mg)Se barriers with about 50 nm thickness. The real QW widths were derived from reflection high energy electron diffraction (RHEED) measurements. Further details on the growth and properties of such samples are described elsewhere [19].

Microdisks were fabricated from these quantum well structures with different CdSe thicknesses via electron beam lithography (EBL) and wet chemical etching (WE) methods. At first, $3-4\,\mu$m thick ring apertures were defined into a 950K PMMA positive resist. After the development, the structure was transferred into the samples by WE using a $K_2Cr_2O_7$+HBr+H_2O solution. Subsequently, selective WE of the (In,Ga)As was performed in a NaOH+H_2O_2 solution. Note that the special ring structure we designed was required to prevent the solution from etching the whole surface, resulting in cracking and flaking off of the (In,Ga)As sacrificial layer. We attribute this behavior to arise from a faster etching process at dislocations in the relaxed (In,Ga)As layer. As the release of the (In,Ga)As material is also accompanied by

#246877 Received 28 Jul 2015; revised 24 Sep 2015; accepted 24 Sep 2015; published 29 Oct 2015

a strong bubble formation, these bubbles are most likely responsible to trigger the disastrous splintering of the sacrifice layer we observed in fully etched samples without the ring apertures.

The photoluminescence (PL) spectroscopy was performed in a confocal μ-PL setup geometry and the luminescence was collected perpendicularly to the surface. A laser with a wavelength of $\lambda = 377$ nm was used for excitation and focused onto the surface down to a spot of about $2\,\mu$m in diameter. It was positioned close to the edge of the microdisk where the whispering gallery modes (WGM) are localized. For all measurements presented here, the excitation power was about $20\,\mu$W. The luminescence was dispersed in a spectrometer with 500 mm focal length and detected by a LN_2-cooled CCD camera.

3. Results and discussion

Figure 1 shows a collection of scanning electron micrograph (SEM) images of a selected microdisk. It has a diameter of about $2.5\,\mu$m and is undercut to remain the free-standing CdSe/ZnSe/(Zn,Mg)Se quantum structure on an (In,Ga)As post of about $1\,\mu$m diameter (see Fig. 1(a)). The surface of the microdisk is relatively smooth, yielding a typical root mean square roughness of the disk surface of about 11 nm as measured by atomic force microscopy ($2\,\text{x}2\,\mu$m scan field, not shown here). A close-up view of the sidewalls in Fig. 1(b) indicate square edges with a moderate surface roughness, which may limit the quality factor of the disk because of scattering losses. The SEM of the edge of the disk also reveals a small region in the center being brighter than the surrounding regions. This corresponds to the CdSe QW while the darker regions are the enclosing ZnSe and (Zn,Mg)Se layers. Figure 1(c) displays an overview of the device geometry. The microdisk is surrounded by a trench that remains from the ring-aperture. This geometry was chosen to ensure a controlled undercut etching. The triangles at the top and bottom border of Fig. 1(c) are markers used for reproducible locating of the microdisks.

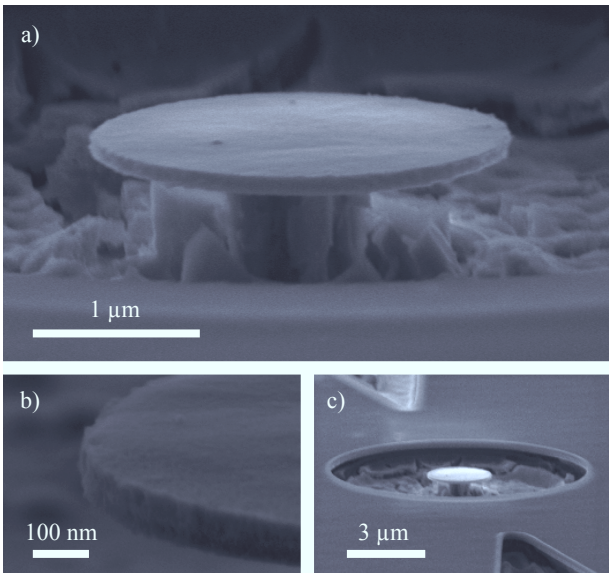

Fig. 1. Scanning electron micrographs of a (Zn,Mg)Se/ ZnSe/CdSe QW microdisk taken at an angle of 77° to the surface. (a) Microdisk on an (In,Ga)As post with cliffy undercut area. (b) Close-up view of a microdisk edge with distinguishable central CdSe QW region. (c) Overview screen of the device geometry to ensure controlled undercut etching.

The optical properties of the manufactured microdisks were analyzed by confocal μ-PL

#246877 Received 28 Jul 2015; revised 24 Sep 2015; accepted 24 Sep 2015; published 29 Oct 2015

spectroscopy at ambient temperature. According to the different widths of the CdSe QWs ($0.9-5.6$ ML measured by RHEED), the ground state transition energy is red-shifted and almost covering the whole visible spectral range. As shown in Fig. 2, the thinnest QW (0.9 ML) exhibits the narrowest emission with a central wavelength of around 2.68 eV in the blue spectral range. The emission of the 3.0 ML sample is centered at ~ 2.47 eV. The luminescence of the two thickest QW samples with 4.7 ML and 5.6 ML CdSe is further red-shifted to ~ 2.3 eV and ~ 2.05 eV, respectively. It should be noted, that these QW thicknesses cannot be realized on standard (001)-GaAs substrates without the strain engineering technique [19], as the strain in the CdSe (e.g. lattice mismatch ~ 6.7 % to GaAs) causes the formation of quantum dots for CdSe layers exceeding 2.1 ML [24, 25]. The observed broadening of the line width of the QW emission with increasing CdSe thickness is related to the inhomogeneous and thickness-dependent strain situation in the heterostructures. More detailed discussion of this effect can be found in Ref. [19].

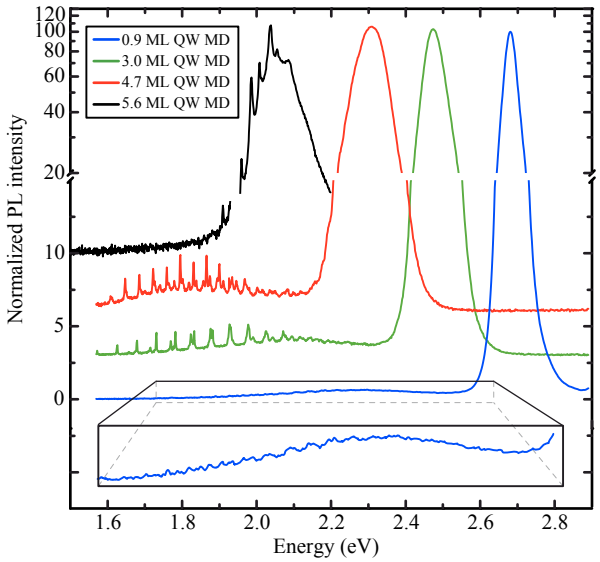

Fig. 2. PL spectra at ambient temperature of (Zn,Mg)Se/ZnSe/CdSe microdisks with different CdSe quantum well thicknesses of 0.9 ML (blue), 3.0 ML (green), 4.7 ML (red) and 5.6 ML (black). The QW emission is shifted from ~ 2.68 eV (0.9 ML) to ~ 2.05 eV (5.6 ML). WGMs can be observed in all spectra for photon energies below ~ 2.3 eV.

Besides the luminescence from the CdSe QW ground-state transition, all spectra in Fig. 2 exhibit a broad and relatively weak emission at lower energies arising from deep level defects. For each sample whispering gallery modes (WGMs) are observed in the lower energy spectal region ≤ 2.3 eV, either covered by the QW luminescence or the deep-impurity band. The missing of the WGMs in the spectral region ≥ 2.3 eV may be attributed to strong damping via photon re-absorption close to the ground state transition, and also at larger energies, due to the nearby band edge of the ZnSe and (Zn,Mg)Se layers. Since the re-absorption strongly depends on the wavelength, it is significantly reduced for the defect band luminescence and for the emission from the 5.6 ML CdSe QW. Although, the CdSe QWs are very thin and therefore provide a small absorption cross-section in the microdisk, the light is guided several times through the circumference of the disk, most likely leading to the increased photon loss. The

#246877 Received 28 Jul 2015; revised 24 Sep 2015; accepted 24 Sep 2015; published 29 Oct 2015

overall extinction $\alpha_{\text{comb.}}$ can be described by

$$\alpha_{\text{comb.}}(\lambda) = \alpha_{\text{scat.}}(\lambda) + \alpha_{\text{re-ab.}}(\lambda) + \alpha_{\text{self-ab.}}(\lambda) \tag{1}$$

The three contributions in Eq. (1) are self-absorption in the CdSe QW ($\alpha_{\text{self-ab.}}(\lambda)$), scattering at the rough surface of the disk ($\alpha_{\text{scat.}}(\lambda)$) and re-absorption in the whole CdSe/ZnSe/(Zn,Mg)Se quantum structure during the wave propagation in the disk ($\alpha_{\text{re-ab.}}(\lambda)$). With increasing QW width, the luminescence is significantly shifted towards lower energies. Therefore the fraction of re-absorption is reduced, while the self-absorption by the thicker CdSe layers is slightly increased. Both effects together may lead to an reduced overall extinction of the modes at lower energies. Consequently, WGMs are mainly obtained in the emission of the 4.7 ML and 5.6 ML thick CdSe QW samples. However, the modes in the central-peak emission (about 2.3 eV) of the 4.7 ML QW are weak and only noticeable as slight intensity modulations at the low energy side, while the modes are much stronger in the deep defect-band region (around 1.8 eV). Quality factors of the WGMs are not exceeding values of 700 as the sidewalls of the microdisks are substantially rough and the (In,Ga)As post diameters are partly inhomogeneous (compare Fig. 1). Both affect the guiding and trapping of the light inside the disks as scattering losses are caused by the wet chemical structuring process. The absence of the WGMs in the central-peak emission of the two thinnest CdSe samples is attributed to the increased self-absorption. We consider the latter contribution as the dominating effect which leads to the complete damping of the WGMs for photon energies ≥ 2.3 eV for all of the samples. In the following a closer analysis of the optical properties such as the dispersion of the material system and the observed losses is performed.

The refractive index of such thin multilayer structures is difficult to measure directly. However, it can be derived from the resonances of the microdisks using the approximation of a closed lightpath with the circumference of the corresponding disk as demonstrated for ZnO based microdisks [26]:

$$n_{\text{eff}}(E) \approx \frac{hc}{2\pi R \Delta E} \tag{2}$$

Here the effective refractive index (n_{eff}) of the disk is calculated from the energetical spacing (ΔE) between consecutive WGMs of the same order and the radius R of the corresponding disk as extracted from the SEM images. Please note: Light waves will not propagate exactly at the outside margin but inside of the material. This fact can easily be considerd by the corresponding reduction of the radius R.

For selected microdisks fabricated from the three thickest CdSe QW samples (3.0 ML, 4.7 ML, 5.6 ML) the derived values of the effective refractive index are presented in Fig. 3(a). For reference, the literature values of the relevant materials in our samples are also included in Fig. 3(a): The refractive index of the QW material CdSe [27] is printed as dotted line. For the (Zn,Mg)Se barriers with ~ 12 % magnesium content the refractive index dispersion was calculated based on the information provided by Liu *et al.* [27]. For comparison only, the refractive index of the binary materials MgSe and ZnSe are also shown. The main fraction of the overall sample thickness of the CdSe/ZnSe/(Zn,Mg)Se QWs (~ 115 nm) is contributed by the two 50 nm thick barriers of (Zn,Mg)Se which have only a slightly smaller refractive index than pure ZnSe. Therefore one might assume that the experimentally derived effective refractive index n_{eff} is similar to that of (Zn,Mg)Se as well.

However, we observed a strong energetically dependent deviation of the data in Fig. 3(a) from the calculated dispersion of the (Zn,Mg)Se. Especially a significantly higher slope of the dispersion of n_{eff} is clearly observed. For energies below 2.0 eV, the refractive indices of all three samples are smaller than that of the (Zn,Mg)Se barriers: We attribute this behavior due to the localization of a substantial fraction of the electric field amplitude of the wavefunctions

#246877 Received 28 Jul 2015; revised 24 Sep 2015; accepted 24 Sep 2015; published 29 Oct 2015

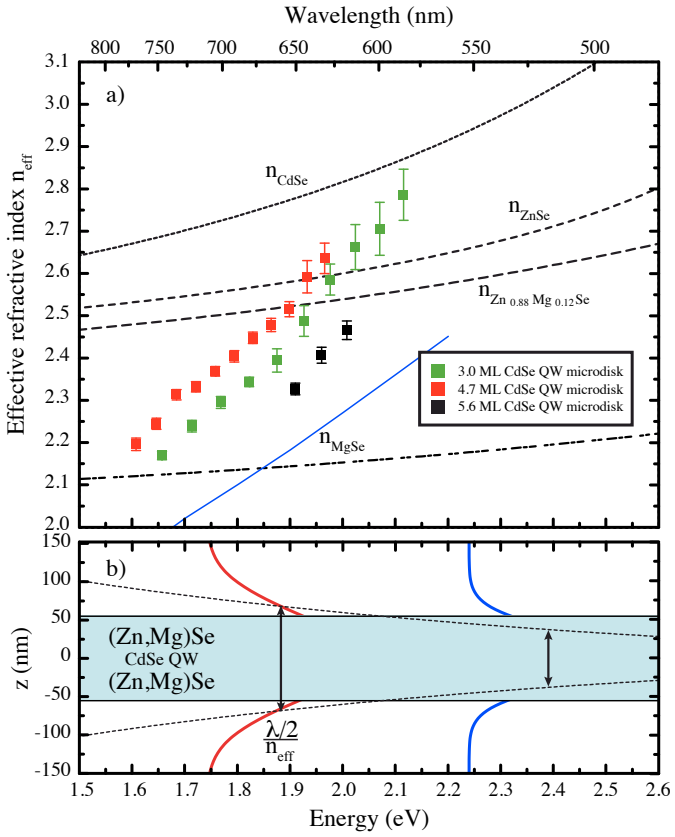

Fig. 3. (a) Effective refractive indices of the microdisks with different CdSe quantum well thicknesses of 3.0 ML (green), 4.7 ML (red) and 5.6 ML (black) in dependence of the photon energy. The black dashed and dotted lines show the refractive index characteristics of the relevant materials. The blue line corresponds to the dispersion of the refractive index $n_{\text{theo.}}$ as calculated according to a model considering the exterior field distribution of the mode across the disk (see text). (b) Mode diameter along the cross-section (i.e. growth direction z) coordinate of the microdisk as a function of the photon energy of corresponding WGMs (dashed line) for which a Gaussian field distribution along the growth direction was assumed (red, blue curves) and the fixed total thickness d of a CdSe/ZnSe/(Zn,Mg)Se quantum structure (light blue area).

in the free-space outside the cross-section of the microdisk. With increasing photon energy the fraction of the evanescent field is continuously reduced: For a small energy interval around 2.0 eV the experimental data of n_{eff} coincide with n_{ZnMgSe} of the (Zn,Mg)Se barriers, which suggests a complete localization of the wavefunction inside the microdisk. For even larger energies, the effective refractive indices change to a more ZnSe- and CdSe-like behavior. The latter can be explained due to further compression of the field amplitude inside the structure and increasing waveguiding within the ZnSe cladding layers and the CdSe QW itself (both with a larger refractive index than that of the (Zn,Mg)Se barriers).

We performed a more detailed quantitative analysis of the above described trends by assuming a Gaussian mode profile of the WGMs along the cross-section of the microdisk (i.e. growth

#246877 Received 28 Jul 2015; revised 24 Sep 2015; accepted 24 Sep 2015; published 29 Oct 2015

direction z) given by

$$E(z) \sim e^{-\frac{z^2}{w^2}} \tag{3}$$

with

$$w = \frac{\lambda}{4 \cdot n_{\text{eff}}} \tag{4}$$

defined as the half-width (in nanometers) for which the amplitude of the field distribution of the WGM drops below the fraction $1/e$ of its maximum. Figure 3(b) illustrates the mode profile of two selected modes with $\lambda = 750$ nm (red curve) and $\lambda = 550$ nm (blue curve), respectively, versus the cross-section coordinate z of the microdisk together with the real dimension of a CdSe/ZnSe/(Zn,Mg)Se quantum structure (light blue area). The dotted line reflects the dependence of the above defined mode diameter w versus energy as calculated based on the experimentally obtained n_{eff} values in Fig. 3(a). For energies below 2.1 eV the mode diameter is clearly larger than the thickness of the quantum structures, which confirms the presence of a substantial evanescent field amplitude in the free-space outside the disk.

According to this result one can describe the trend of the observed dispersion in Fig. 3(a) of n_{eff} by a weighted average approximation which considers the relative integral mode amplitude inside (i.e. with refractive index n_{ZnMgSe}) and outside the microdisk (i.e. with refractive index $n_0 = 1$ in air), respectively:

$$n_{\text{theo}} = \frac{A_{\text{in}}}{A_0} * n_{\text{ZnMgSe}} + \left(1 - \frac{A_{\text{in}}}{A_0}\right) * n_0 \tag{5}$$

Here A_{in} is the integral mode amplitude within the limits $z = -d/2$ and $z = +d/2$ of the overall thickness d of the quantum structure and A_0 the corresponding full mode amplitude over the whole z-space. The blue line in Fig. 3(a) reflects the dispersion of n_{theo} as a function of the energy and within the valid range of our model. The offset between the absolute values of n_{eff} and n_{theo} might be due to a slightly different refractive index dispersion of (Zn,Mg)Se in our samples compared to that after Liu *et al.* [27]. Apart from that, the trend and relatively good agreement between the experimentally derived refractive indices n_{eff} of the disks and the calculated dispersion is clearly visible. This confirms our self consisting model approach based on a mode profile of the WGMs with a substantial evanescence field. However, the significant deviation of the curves with increasing photon energy reflects a raising influence of the CdSe QW layer on the effective refractive index dispersion.

As previously discussed, we observed strong damping of the WGMs for energies ≥ 2.3 eV that is most likely limited by self-absorption of photons in the CdSe QW. Considering the generation/recombination mechanism of excitons in the WGMs, the peaks are arising from the luminescence by resonant amplification. The peak height is then limited by the sum of the losses. As just the losses by absorption are substantially depending on the photon energy, we find the peak intensity correlated to the absorption. We quantified this by the ratio κ between the integrated luminescence intensity of the background versus the integrated intensity of the WGM peak within the same spectral interval, providing qualitative information about the extinction coefficient: The latter is proportional to the background to peak ratio of the recorded PL-spectra.

For selected WGM modes of the samples we performed this analysis and the results are plotted as a function of the photon energy in Fig. 4 for the three thickest CdSe QWs. Contrary to the effective refractive index, the extinction coefficient is correlated to the QW width. For low photon energies (≤ 1.9 eV), the intensity ratio κ is almost constant. At higher photon energies, it strongly increases and was fitted by linear functions for all analyzed QW samples. The photon energy at the cross sections of the appropriate two linear fits can be associated with the bandgap energy of the semiconductor material. The different extracted edge energies of 1.93 eV (5.6 ML

#246877 Received 28 Jul 2015; revised 24 Sep 2015; accepted 24 Sep 2015; published 29 Oct 2015

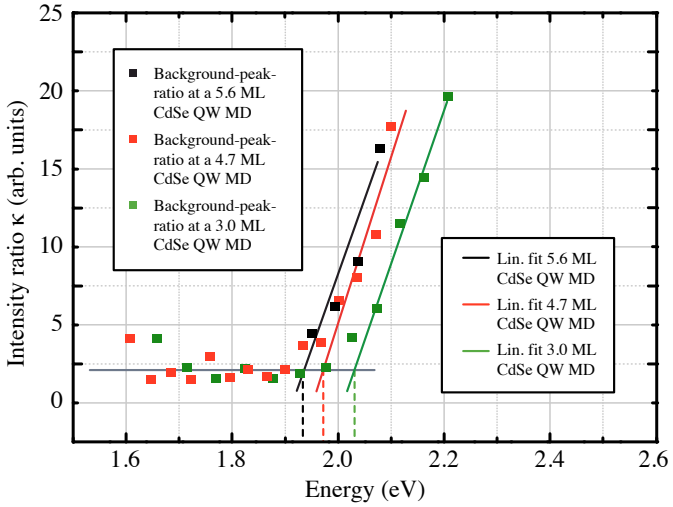

Fig. 4. Extinction coefficients derived by the proportional background to peak ratio of the 3.0 ML (green), the 4.7 ML (red) and the 5.6 ML (black) CdSe QW microdisk as well as their corresponding linear fits in the rising regions. The cross-section between the two linear trends is associated with the bandgap energy.

CdSe (black)), 1.97 eV (4.7 ML CdSe (red)) and 2.03 eV (3.0 ML CdSe (green)) are related to the CdSe QW width and denote the same trend as that of the PL spectra in Fig. 2: In comparison to pure CdSe ($E_{\mathrm{gap}} \sim 1.68$ eV) [27], all bandgap values we extracted from Fig. 4 are slightly higher and increase with decreasing well width. Due to the significantly higher band gap energies of the embedding materials ZnSe ($E_{\mathrm{gap}} \sim 2.72$ eV) and (Zn,Mg)Se ($E_{\mathrm{gap}} \sim 2.89$ eV) [27], no substantial increase of absorption is expected in the relevant investigated spectral range in Fig. 4. This supports our above discussed assumption that the absence of WGMs in the energy region above 2.3 eV mainly stems from the self-absorption of photons in the CdSe QWs.

4. Conclusions

For the first time, photonic microcavities from strain-compensated CdSe/ZnSe/(Zn,Mg)Se heterostructures as a basic device for modern quantum applications were successfully realized. The fabricational issues of anisotropic (In,Ga)As undercut etching were solved by a special ring mask design of the resist, preventing the guiding layer structure from cracking and flaking off of the sacrificial layer as caused by the formation of bubbles in the etching solution.

We clearly observed whispering gallery modes in the photoluminescence spectra of the fabricated CdSe/ZnSe/(Zn,Mg)Se quantum well microdisk cavities in the red and yellow spectral range ($\sim 1.6 - 2.3$ eV) at ambient temperature. The spectral dependent intensity reduction and finally the absence of whispering gallery modes for higher photon energies was attributed to an unusual strong self-absorption of photons in the CdSe QWs. The latter was analysed by calculation of the spectral change of the ratio of the integral intensities of background and mode photoluminescence. Our findings revealed an absorption threshold that is close to the corresponding transition energies of the thickness-dependent ground state transitions in the CdSe QWs. Future work will be focused on the reduction of the strong re-absorption effect.

The dispersion of the effective refractive index of the microdisk cavities was calculated only from the mode spacing and based on the assumption of a Gaussian mode amplitude distribution along the cross-section of the microdisks. This model allows for fast and elegant estimation of

#246877 Received 28 Jul 2015; revised 24 Sep 2015; accepted 24 Sep 2015; published 29 Oct 2015

the effective refractive index dispersion in a complex multilayer structure. We obtained significantly smaller refractive indices as those of the materials in the layers, which revealed a reduced mode field confinement in the microdisks and a substantial evanescent field. The latter is an important aspect for efficient photon-extraction from the microdisk cavities and photon-guiding via a nearby located integrated optical waveguide slab. The results presented here form a firm basis for the development of photonic interconnection of several microdisks in this material system as desired for modern quantum applications, for example, integrated optically connectable light sources.

Acknowledgments

This work was funded by the Volkswagen Foundation (Project No. 88360/90080) and by the Deutsche Forschungsgemeinschaft (DFG) (Project LI668/8-1). We further acknowledge the financial support by the DFG and the Russian Foundation of Basic Research in the frame of the ICRC TRR 160. S.S., A.L. and A.D.W. acknowledge gratefully support of Mercur Pr-2013-0001, BMBF - Q.com-H 16KIS0109, and the DFH/UFA CDFA-05-06.

#246877 Received 28 Jul 2015; revised 24 Sep 2015; accepted 24 Sep 2015; published 29 Oct 2015